SINGULARITIES AND PHYSICS OF TURBULENT SHEAR FLOWS

Bérengère Dubrulle
SPEC, CEA, CNRS,
University Paris-Saclay,
CEA Saclay,
Gif-sur-Yvette, France
berengere.dubrulle@cea.fr

Lucas Fery
SPEC, CEA, CNRS,
University Paris-Saclay,
CEA Saclay,
Gif-sur-Yvette, France

Adrien Lopez
SPEC, CEA, CNRS,
University Paris-Saclay,
CEA Saclay,
Gif-sur-Yvette, France

Wandrille Ruffenach
SPEC, CEA, CNRS,
University Paris-Saclay,
CEA Saclay,
Gif-sur-Yvette, France

ABSTRACT

Turbulence, a phenomenon observed by physicists in natural and laboratory flows, is thought to be described by Navier-Stokes equations (NSE). Yet, it is not yet known whether the Cauchy problem is well posed for these equations, and whether solutions of finite energy are regular or unique. In the physics community, the ”singularity hypothesis” is generally discarded, following the reasonable principle that ”singularities are a mathematical curiosity, in nature they do not exist”.

In this lecture, we discuss how recent progresses in mathematics, numerical simulations and laboratory experiments changed such simple vision leading to a new picture where quasi-singularities living beyond Kolmogorov scale play a central role. We describe specific application to the case of flow near boundaries, and show how to interpret energy balance, dissipation scaling and statistics, as well as velocity profiles using a model based on elementary singularities as building blocks.

1 Empirical laws of geophysical flows near boundaries

An instantaneous snapshot of a turbulent flow, such as the ocean near the coast of Florida (figure 1-(A)) displays many complicated features, such as eastwards jets, or small scale coherent structures (figure 2-(A)), each of them bearing striking empirical properties.

1.1 Jets

Jets are an important component of the Earth system, because of they carry heat, and nutrition that are essential for marine life or human activities (plankton, fishery,..). Two famous example are the Gulf Stream, near the coast of Florida, or the Kuroshio, near the coasts of Japan (figure 1-(A)). They originate from western boundary currents that penetrate deep into the Ocean (figure 1-(B)), thinning into jets that shed perpetually small scale vortices (figure 2-(A)).

1.2 Coherent structures

Small scale structure carry in fact most of the energy in the ocean, as can be seen in figure 3-(A), that shows the energy of the mean and random components for various viscosities. In the same way, the energy dissipation is due mainly to the random component, as soon as the viscosity is small enough, see figure 3-(B). The difference between mean and random components reveals the spatial heterogeneity of the dissipation, as

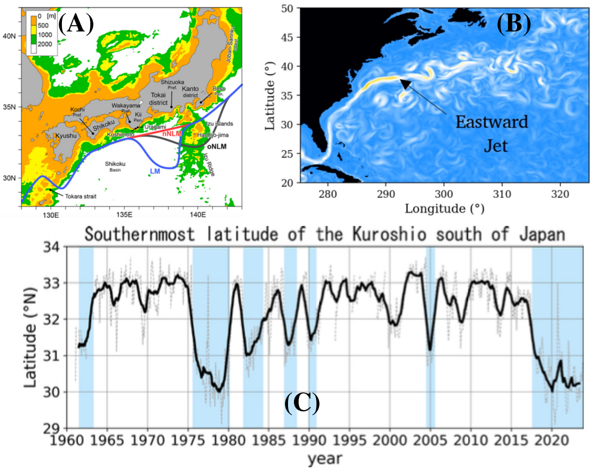

Figure 1. Instantaneous oceanic turbulent flows near coasts. (A) near the Japan coast: the Kuroshio current and its wandering. (B) near the Florida coasts, obtained though the Copernicus Global Ocean Reanalysis dataset. Credits: Lellouche *et al.* (2018); Miller (2025);(C) Historical record of the Kuroshio wandering.

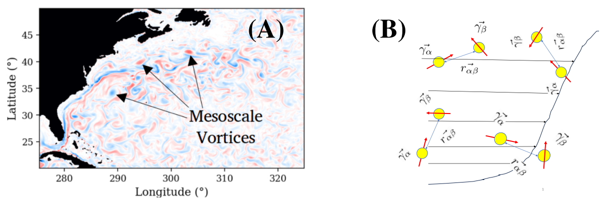

Figure 2. (A) Small scale coherent structures near the Florida coasts, as revealed by the fluctuations of the vorticity field. Credits: Lellouche *et al.* (2018); Miller (2025). (B) Vorton model of turbulence.

can be seen by looking at a map of the dissipation in the ocean obtained in a global ocean model by Pearson & Fox-Kemper (2018), see figure 4-(A). One sees that the dissipation is more intense near some, but not all coasts, and is distributed into large scale elongated structures. With good eyes, you should be able to see that dissipation is more intense inside small scale vortices, see Pearson & Fox-Kemper (2018). Such heterogene-

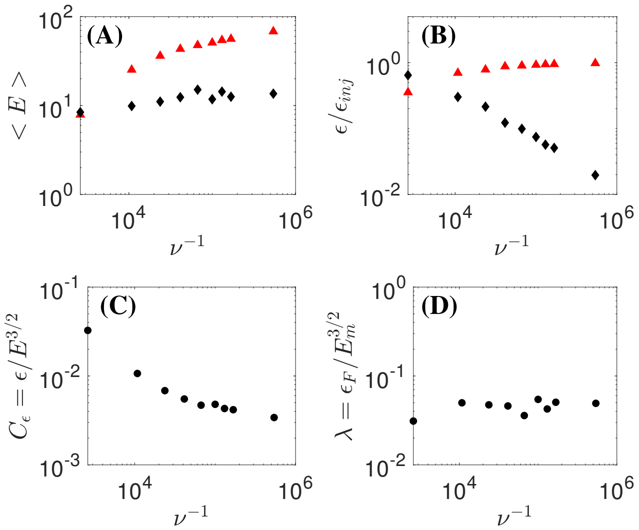

Figure 3. Energy and dissipation observed in simulations of ocean turbulence near a coast. (A) Energy contained in the mean flow (black diamonds) and random fluctuations (red triangles) and (B) Fraction of energy dissipation due to mean flow (black diamonds) and random fluctuations (red triangles) as a function of viscosity.(C) Dissipation anomaly and (D) friction. After Miller (2025).

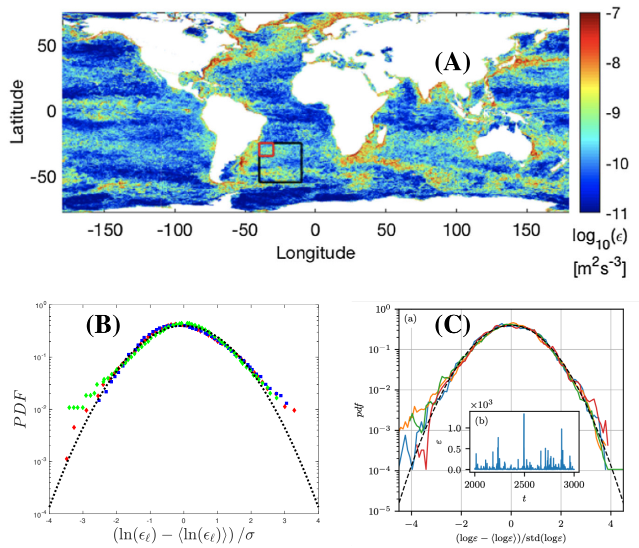

Figure 4. Statistical properties of dissipation (A) Map of the dissipation in a global Ocean model. Credits: Pearson & Fox-Kemper (2018). (B) Probability distribution function of dissipation in the global ocean model.The three different color correspond to different region of dissipation: red: global; blue: $30° \times 30°$ (black square in Fig. 2-(A)); green $10° \times 10°$ (red square in Fig. 2-(A)). After Pearson & Fox-Kemper (2018). (C) Probability distribution of the dissipation in the vorton model. The black dotted line is a Gaussian of unit variance. The insert shows the instantaneous value of the dissipation, evidencing large fluctuations. Credits: Ruffenach *et al.* (2025); Fery (2025)

ity produces a log-normal distribution for the dissipation, see figure 4-(B). This distribution is universal for the centered reduced variable in region where the dissipation is the highest, as it does not depends on where the statistics is taken.

2 Mysteries associated with the ocean turbulence

2.1 Where do the vortices come from?

A first mystery lies in the origin of small scale vortices. Indeed, ocean, like any geophysical flows, are characterized by very large Reynolds number. In this limit, the flow equations tend to Euler equations, which bears many conservation laws. Among them, Kelvin theorem states that vorticity should be conserved. In that situation, how can we create vortices efficiently?

2.2 What kind of limit for dissipation?

A close inspection of the dissipation in the fluctuating component of the ocean, figure 3-(B), shows that the dissipation seems to saturate, or at least grow very mildly when $\nu \to 0$. In the same time, the energy of the fluctuating component seems to grow without limit, indicating diverging velocities, and, so, a singularity. A first problem is to understand the origin of such singularity. A second problem is to quantify its influence on the dissipation, which is dominated by the dissipation from fluctuation ε_F . On dimensional ground, we can link the dissipation ε and the energy E through $\varepsilon = E^{3/2}/L$, where L is a characteristic scale. This means that increasing energy automatically increases energy dissipation, at fixed L. So,by considering normalized dissipations, we can remove the influence of energy on the dissipation, and investigate finer mechanisms.

2.2.1 Dissipation(s)

Let us start by considering the influence of the energy of the fluctuation E_F, and build the reduced dissipation $C_\varepsilon = \varepsilon/E_F^{3/2}$, where ε is the total energy dissipation. This is shown in Figure 3-(C). One observes two regime: at large viscosity $\varepsilon/E^{3/2} \propto \nu$. This corresponds to a *laminar regime*, where all dissipation is produced by viscosity. At small viscosity, we observe a second power-law $\varepsilon/E^{3/2} \propto \nu^{1/4}$. This is puzzling, as it indicates the presence of a new mechanism to dissipate energy. Which one is a mystery to be solved.

2.2.2 Friction law

We can now consider the influence of the energy of the mean flow E_m onto the dissipation by computing the friction factor $\lambda = \varepsilon_F/E_m^{3/2}$. This is shown on figure 3-(D). One sees that it is approximately constant for any viscosity, meaning that we can interpret λ as the friction (drag) exerted by small scale over the large scale. This mysterious property is very useful when considering appropriate models of geophysical flows, or for flow near wall, as it enables to parametrize the influence of the small scale.

2.3 Log-normal law and diverging dissipation

Figure 4-(B) shows that the dissipation distribution is log-normal. Log-normal laws are pathological in the following sense: imagine you want to define a typical dissipation $\varepsilon_p = \frac{<\varepsilon^{p+1}>}{<\varepsilon^p>}$, where the average is taken over the statistics of ε. For $p = 0$, $\varepsilon_0 = <\varepsilon>$, a typical value near the summit of the PDF. As p increases, ε_p traces values of ε that are rarer, and located

further and further in the tail of the PDF. For a log-normal law, we have $< \varepsilon^p >\sim< \varepsilon >^p \exp(\mu p(1-p)/2)$, where $\mu > 0$ is connected to the variance of the distribution. So, the quantity ε_p growth like $\exp(\mu p)$, that diverges in the $p \to \infty$ limit. This is another indication of singularities plaguing our problem.

2.4 Breaking of unicity

Being instantaneous structures, the jet are not stationary and their amplitude and location may significantly vary. Figure 1-(B) and (C) shows an illustration of the possible wandering of the Kuroshio, as well as the statistics of its southern most part. Such statistics are suggestive of a bistable system, meaning that there is not unicity of solution for turbulence. Given that turbulence obeys partial differential equations (Navier-Stokes equations), this means that some singularities are present to prevent unicity of solutions to apply.

3 Singularities in flows near boundary

We saw previously many empirical laws suggestive of a singular behaviour in flows near boundaries. There are actually a number of mathematical results that explain such behaviour.

3.1 Prandtl equations

As recognized by Prandtl (1905), if the boundary condition is of no-slip type (vanishing of the tangential velocity at the wall), it favors the development of a boundary layer thinning with decreasing viscosity like $\nu^{1/2}$, making capture of this phenomenon at very large Reynolds number *Re* out-of-reach of present numerical simulations. These difficulties motivated another type of approach, through asymptotic expansions of the equation of motions, using the size of the boundary layer as a small parameter. This approach was initiated by Prandtl himself, resulting in the Prandtl equations that couple an inviscid bulk described by Euler equation, with a boundary flow piloted by the tangential velocity. In the simplest 2D setting, they read (Collot *et al.*, 2021):

$$\begin{aligned} \partial_t u_x + (u\cdot\nabla)u_x &= \nu\Delta u_x, \\ \partial_x u_x + \partial_y u_y &= 0, \\ u(x,t=0) &= u_0(x). \end{aligned} \tag{1}$$

Integration of equations (1) requires boundary conditions. The simplest set of boundary conditions is periodic boundary conditions in the x direction. In the vertical direction, we impose no-slip boundary condition $u_x = 0$ at $y = 0,\infty$ and $p = 0$ at $y = \infty$. When $\nu \neq 0$ solution of such equation develop boundary layer near the wall. However, in the inviscid limit, Prandtl equations (1) with the trivial Euler flow condition at $y = \infty$ experience finite type blow-ups of two types depending on initial conditions (Collot *et al.*, 2021): either a shock at the interface, or a boundary layer detachment. The inviscid blow-up is not generic, in the sense that there are many ways to achieve the blow-up, depending on initial conditions. However, there is a generic, stable one, corresponding to a self-similar blow-up, described by:

$$u_x(t,x,y) = (t_b - t)^{1/2}\Theta\left(\frac{x}{(t_b-t)^{3/2}}, \frac{y}{(t_b-t)^{-1/4}}\right), \tag{2}$$

where Θ is a function and t_b is the blow-up time. This self-similar solution admits stationary (time independent) solutions that are power-laws in x and y, with exponents $h_x = 1/3$ and $h_y = -2$. This results in diverging velocity gradients in the x direction, and diverging velocity in the y directions, thereby explaining some puzzling observations in Figure 3. As later shown by Collot *et al.* (2022), this self-similar blow-up also generically occurs for viscous Prandtl equation with no-slip boundary conditions, provided the viscosity is only in the vertical direction. This mean that the corresponding blow-up solutions is very robust. The corresponding blow-up does not occur at the boundary, nor at a finite distance from the axis, since the singularity is ejected at infinity. This makes interaction with the Euler outflow very likely and results in the breaking of the Prandtl approximation, i.e. Navier-Stokes solutions detaching from Prandtl solutions as the singularity is approached.

3.2 2D Navier-Stokes with no-slip boundary condition

This difference motivates direct simulation of the 2D Navier-Stokes with no-slip boundary conditions. These simulations are delicate, as very large resolutions are required to capture the boundary layer. It can however be done in some simple settings with symmetries, leading to interesting observations. For example, Obabko & Cassel (2002) study boundary layer dynamics via direct numerical solutions of the unsteady Navier-Stokes equations are considered for the flow induced by a thick-core vortex convecting along a surface in a two-dimensional incompressible flow with no-slip boundary condition. The vortex mediates eruption of the boundary layer, resulting later in interaction between the viscous boundary layer and the outer inviscid flow. This interaction was then shown to occur at two length scale (small or large), depending on the Reynolds number: only large scale at small Reynolds number $Re \leq 10^3$ (but with no spike formation), both large and small at moderate Reynolds number, and only small scale at large Reynolds number $Re > 10^5$. A few years later, Gargano *et al.* (2014) analyses possible complex singularities arising in this geometry, and were able to identify 3 groups of complex singularities, corresponding respectively to the Prandtl singularity, and to small or large scale interactions. In the inviscid limit, the 3 complex singularity group have a tendency to fusion, indicating a possible convergency of the inviscid Navier-Stokes solution towards Prandtl solution. Therefore, it seems likely that singularities are present in the inviscid limit, and that they play a role in the boundary layer turbulence.

3.3 Two consequences of the singularities

Singularity produce many pathologies: loss of unicity, divergencies... More interestingly, they produce spontaneous symmetry breaking, and breaking of the associated conservations laws. Two example are time translation and relabelling symmetry.

3.3.1 Dissipation by singularity

The conservation law associated with time translation is energy conservation. Its breaking by singularity can be illustrated using the local energy budget derived by Duchon & Robert (2000) for solutions of the Navier-Stokes equation:

$$\partial_t \frac{\mathbf{u}^2}{2} + \nabla\cdot\left[\mathbf{u}\frac{\mathbf{u}^2}{2} + \mathbf{u}p\right] = -\mathscr{D} - \nu(\nabla u)^2. \tag{3}$$

where $\mathscr{D}$ is defined using velocity increments $\delta\mathbf{u}(\ell) = \mathbf{u}(x+\ell) - \mathbf{u}(x)$ as

$$\mathscr{D} = \lim_{\ell\to 0} \mathscr{D}^{\mathrm{I}},$$
$$\mathscr{D}^{\mathrm{I}} = \frac{1}{4}\int d\xi \left[\nabla\phi^{\ell}\right](\xi)\cdot\delta_{\xi}\mathbf{u}(\delta_{\xi}\mathbf{u})^{2}. \tag{4}$$

This term does not depend explicitly on viscosity. For sufficiently regular velocity fields $\delta\mathbf{u}(\ell) \sim l^{h}$, it vanishes like ℓ^{3h-1}, whenever $h > 1/3$. On the contrary, for $h \leq 1/3$ it can produce a finite energy dissipation, even in absence of viscosity. This condition is satisfied by the Prandtl singularity, so that we have a possible explanation for what we observe in Figure 3-(A) and (B).

3.3.2 Vortex production by singularity

The conservation law associated with relabelling symmetry is the velocity circulation Γ around any closed contour $\mathscr{C}$ advected by the flow. The corresponding circulation balance in the case of irregular flow has been done by Eyink (2006):

$$\partial_t\Gamma = -\mathscr{O} + \nu\oint_{\mathscr{C}}\Delta\mathbf{u}\cdot d\mathbf{s}. \tag{5}$$

where $\mathscr{O}$ is the turbulent vorticity production defined as:

$$\mathscr{O} = \lim_{\ell\to 0}\mathscr{O}^{\mathrm{I}},$$
$$\mathscr{O}^{\mathrm{I}} = \oint_{\mathscr{C}} d\mathbf{s}\int_{\xi<\ell}\left[\nabla\phi^{\ell}\right](\xi)\left[\delta_{\xi}\mathbf{u}\otimes\delta_{\xi}\mathbf{u} - \frac{(\delta_{\xi}\mathbf{u})^{2}}{2}\bar{\bar{\mathbf{I}}}\right]. \tag{6}$$

This term is independent of viscosity. It scales like ℓ^{2h-1} so it can lead to vorticity production/destruction by irregular field as soon as $h \leq 1/2$. Prandtl singularity enters this category. By nature singularities (or quasi-singularities if they are regularized by viscosity) act at very small scale. This vorticity production by singularities therefore provides an explanation of the small vortices proliferation observed in Figure 2-(A). They are generated at the boundary, and then swept away by the boundary layer vertical instability.

3.3.3 Bifurcations through singularities

Being able to break symmetries, singularities are also natural catalyzers of bifurcations. This phenomenon is difficult to explore numerically as it requires very large resolution. It can however be captured by simplified model of turbulence, in which the scales are decimated in a logarithmic manner. Such models are called: fluids on log-lattice, and have been invented by Campolina & Mailybaev (2018); Campolina (2022). They consist in projection of the equations onto an exponentially spaced Fourier grid, a procedure that allows to retain all symmetries and conservation laws of the original equations, at the expenses of neglecting non-local interactions. The adaptation of this to flow with boundary has been done in Campolina & Mailybaev (2025); Lopez (2026); Lopez & Dubrulle (2026). It allows to treat the case of flows with Navier-slip boundary conditions, and explore their dynamics for a wide range of parameters. Figure 5-(B) shows the time-evolution of the drag force for an incompressible fluid with velocity $\mathbf{u}(\mathbf{x},\mathbf{y},\mathbf{t})$ on a half-plane domain $y \geq 0$ with a flat boundary at $y = 0$ at very low Reynolds number, for different slip conditions, starting from the same initial condition. The fluid obeys 2D Navier-Stokes equations

$$\partial_t\mathbf{u} + (\mathbf{u}\cdot\nabla)\mathbf{u} = -\nabla p + \nu\Delta\mathbf{u},$$
$$\nabla\cdot\mathbf{u} = 0, \tag{7}$$

subject to the Navier-slip boundary conditions:

$$\nu\partial_y u_x = \hat{\alpha}u_x, \tag{8}$$

where $\hat{\alpha} \in [0, +\infty]$. This boundary condition allows to interpolate between stress free boundary conditions ($\hat{\alpha} = 0$) and no slip boundary conditions ($\hat{\alpha} = +\infty$). Due to the boundary condition, the energy dissipation is produced by two terms (Lopez & Dubrulle, 2026):

the bulk dissipation $\varepsilon = \nu < (\nabla\mathbf{u})^2 >$
the boundary layer dissipation $\varepsilon_{\alpha} = \hat{\alpha}\int dx|u_x|^2$.

In the no-slip limit, the log-lattices simulations reproduce many of the features of the full simulations of Ocean near Florida coast by Miller (2025). The total kinetic energy E is increasing with Reynolds number Re (figure 5-(A)). The non-dimensional bulk energy $\varepsilon/E^{3/2}$ is mildly decreasing with Re (figure 5-(C). However, due to the weak numerical costs of log-lattice simulations, we can explore a range of parameters that are not accessible to direct numerical simulations, and thus, evidence new features in the inviscid limit $\nu \to 0$ or the no-slip limit $\hat{\alpha} \to \infty$.

For example, as seen in Figure 5-(B), the drag force displays two regimes in the inviscid no-slip limit: a low fluctuating regime, where the drag is independent of the slip condition $\hat{\alpha}$. A high fluctuating regime, which appears more stochastic. This change of regime (a bifurcation) was shown to be associated to a singularity occurring in the inviscid limit (Lopez & Dubrulle, 2026). Associated to this singularity is a switch between a deterministic regime, where the dynamics is entirely piloted by the initial conditions, and a stochastic regime, which is associated with the phenomenon of spontaneous stochasticity, found in many non-linear systems (Mailybaev & Raibekas, 2023), shell models (Mailybaev, 2016; Bandak *et al.*, 2024), Kraichnan model (Falkovich *et al.*, 2001), Burgers equations (Eyink & Drivas, 2015) and 2D singular shear flows (Thalabard *et al.*, 2020).

Physically, this bifurcation corresponds to a transition between a laminar boundary layer regime, to a turbulent boundary layer regime. When forcing at fixed value of viscosity, the bifurcation is only one way, with no possibility to switch alternatively between the two regimes, like in Figure 1-(C). In most natural flows however, the forcing rather corresponds to fixed values of the (heat, momentum, energy,..) flux. This means forcing along horizontal lines in figure 5-(D), rather than along vertical lines. For certain values of the imposed flux, this means that there is a range of viscosity where the system is in the "forbidden zone", a zone of the parameter space which is inaccessible when forcing at imposed viscosity. In that forbidden zone, the system can become bistable, alternating between the laminar and turbulent regime. A dynamics like this has already been observed e.g. in the von Karman flow, when forcing at constant torque in the forbidden zone (Saint-Michel *et al.*, 2013).

A similar mechanism could therefore explain what is observed in Figure 1-(C).

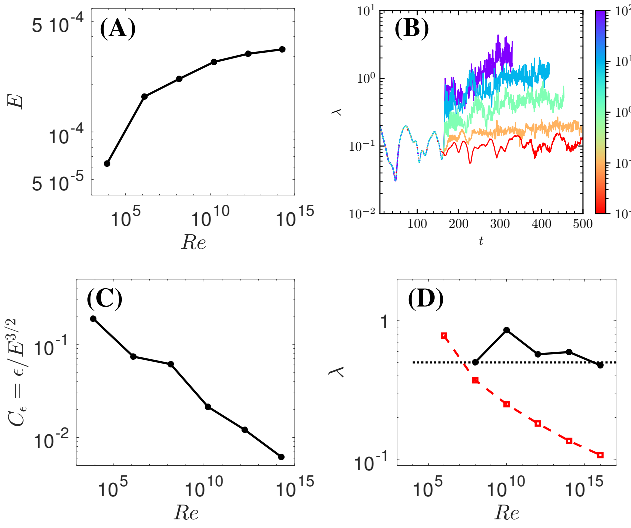

Figure 5. Numerical simulation of 2D Navier-Stokes equations over a flat boundary using log-lattices. After Lopez (2026). (A) Total energy, as a function of the Reynolds number. (B) Instantaneous boundary layer drag ε_α as a function of time, for various slip parameters $\hat{\alpha}$ (coded in color) in the inviscid limit. (C) Non dimensionalized bulk dissipation $C_\varepsilon = \varepsilon/E^{3/2}$ (D) Mean non-dimensionalized drag $\lambda = \sqrt{\hat{\alpha}\varepsilon_\alpha}/E$ in the no-slip limit, showing the two regimes before (red squares, laminar) and after blow-up (black star, turbulent). The forbidden zone corresponds to the space in between the red dashed line and the black continuous line. A forcing at constant drag (horizontal dotted line) allows bi-stability between the laminar and the turbulent regime for any $10^8 < Re < 10^{15}$.

4 The vorton model

4.1 Vorton definition

So far, we have found a plausible mechanism of creation of small scale vortices near a boundary layer. The next step is trying to model their influence on the dynamics. Because these vortices are at very small scale, see figure 2-(A), it is natural to assimilate them as point-like singularities, named *vorton* (Novikov, 1983), located at position $\boldsymbol{x}_\alpha$ and with circulation (vorticity times a volume) $\boldsymbol{\gamma}_\alpha$. Physically, these vortons correspond to debris from coherent vortices generated in the viscous sublayer, that penetrate in the overlap region and provide a continuous forcing allowing to reach a statistically steady state. By summing their contribution, they generate a vorticity field of the form

$$\boldsymbol{\omega}(\boldsymbol{x},t) = \sum_\beta \boldsymbol{\gamma}_\beta(t)\delta(\boldsymbol{x}-\boldsymbol{x}_\beta(t)). \quad (9)$$

The velocity field they produce is recovered using Biot-Savart law,

$$\boldsymbol{u}(\boldsymbol{x},t) = -\frac{1}{4\pi}\sum_\beta \frac{\boldsymbol{x}-\boldsymbol{x}_\beta}{\|\boldsymbol{x}-\boldsymbol{x}_\beta\|^3} \times \gamma_\beta, \quad (10)$$

and is by construction divergence-free.

4.2 Vorton equations

Vorton dynamics is obtained through a two way coupling between large-scale shear and the vortons (Nazarenko, 2000; Nazarenko *et al.*, 2000; Ruffenach *et al.*, 2025). On the one hand, the action of large scales onto small scales is described by rapid distorsion theory (RDT), where small scales are advected and sheared by the mean shear. On the other hand, the small scales act on the large scales via the Reynolds stress. Under these assumptions, the resulting vorton equations write:

$$\begin{aligned} \frac{D\boldsymbol{x}_\alpha}{Dt} &= \boldsymbol{u}(\boldsymbol{x}_\alpha,t) + \boldsymbol{U}(\boldsymbol{x}_\alpha,t), \\ \frac{D\boldsymbol{\gamma}_\alpha}{Dt} &= [\nabla\boldsymbol{u}(\boldsymbol{x}_\alpha,t)]^{\mathrm{T}}\boldsymbol{\gamma}_\alpha + [\nabla\boldsymbol{U}(\boldsymbol{x}_\alpha,t)]^{\mathrm{T}}\boldsymbol{\gamma}_\alpha, \\ \partial_t\boldsymbol{U} + \boldsymbol{U}\cdot\boldsymbol{U} &= -\nabla P + \nu\Delta\boldsymbol{U} - \nabla < \boldsymbol{u}\otimes\boldsymbol{u} >, \end{aligned} \quad (11)$$

where $\boldsymbol{U}(\boldsymbol{x}_\alpha,t)$ is the large scale velocity field, $< \boldsymbol{u}\otimes\boldsymbol{u} >$ is the Reynolds stress, and it is understood that the velocity field $\boldsymbol{u}(\boldsymbol{x}_\alpha,t)$ and its gradient $\nabla\boldsymbol{u}(\boldsymbol{x}_\alpha,t)$ are evaluated with EQ. (10) but without the $\alpha = \beta$ term in the sum since vortons cannot self-advect.

Overall, the vorton dynamics is described by a set of ODE, that can be integrated to obtain the coupled dynamics between the vortons and the large scale shear. This dynamics is illustrated in Figure 2-(B).

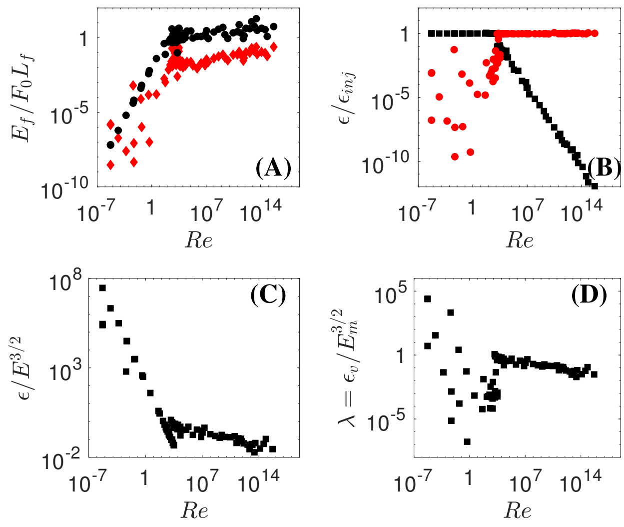

Figure 6. Energy and dissipation observed in numerical simulation of vortons interacting with a mean shear. (A) Energy contained in the mean flow (black diamonds) and random fluctuations (red triangles) and (B) Fraction of energy dissipation due to mean flow (black diamonds) and random fluctuations (red triangles) as a function of viscosity. After Fery (2025). (C)

4.3 Energy and dissipation

As an example, we provide in Figure 6 a few results obtained by integration of the equations for 27 to 125 vortons (Ruffenach *et al.*, 2025; Fery, 2025) taking a simple shear flow: $\boldsymbol{U}(\boldsymbol{x},t) = (a(t)\sin(k_s z), 0, 0)$ as the large-scale. In that case, the coupling with the vortons only influences the amplitude a, and the whole system become a system of ODEs. The model displays an interesting transition between two regimes: (i) a laminar regime, in which all the dissipation is accounted for by the large-scale flow, and the vorton dynamics is essentially diffusive; (ii) a turbulent regime, in which most of the dissipation is produced by the vortons. These two regimes correspond to different scalings of the dissipation and as a function of Reynolds, with power laws that resembles the laws observed in classical turbulence. This results can be confronted to the results obtained full integration of the 2D Navier-Stokes equations with no-slip boundary conditions, namely Fig. 3-(A) and (B) for the energy and the fraction of energy dissipation, and 3-(C) and (D) for the normalized friction and dissipation. We see striking similarities. They also compare well with the results of the log-lattice model, as they capture the same laminar-turbulent transition. The log-normal dissipation statistics are also captured by this model, as shown in Fig. 4-(C).

4.4 Flow profile

The vorton model also allows computation of the flow profile in some simple but classical cases, in geometries where the mean flow is in the x direction, but only depends on z, $\boldsymbol{U}(\boldsymbol{x},t) = (U(z),0,0)$ (Nazarenko *et al.*, 2000). In that case, the large scale equations simply reads:

$$\partial_t U + \partial_t < uw > = -\partial_x P + \nu \partial_z \partial_z U, \tag{12}$$

with stationary solution only depending on the Reynolds stress component $< uw >$. The later can be analytically computed from the vorton RDT dynamics, resulting in $< uw > = \lambda / \partial_z U$. Plugging this results into Eq. (12) results in stationary solutions behaving like $U(z) \sim \log(z)$, which is the classical log-low of the wall.

More generally, when surface term and external forcing are included, the stationary equations in the x direction read:

$$\begin{aligned} \partial_z \langle \overline{U w} \rangle + \partial_z \langle \overline{uw} \rangle &= -\partial_x P + \nu \partial_{zz} U + \overline{\sigma_x} + \mathscr{S}(z), \\ \langle \overline{uw} \rangle &= \nu_t \partial_z U \end{aligned} \tag{13}$$

where ν_t is a turbulent viscosity, given by:

$$\nu_t = \nu_{t*} + \frac{\tau_*}{\partial_z \langle U \rangle} + \frac{\lambda_0 + \eta_0 \langle U \rangle}{(\partial_z \langle U \rangle)^2}. \tag{14}$$

where ν_{t*}, τ_*, λ_0 and η_0 are constants which are different in the near-wall and core regions. Using these, it is possible for example to fit perfectly the velocity profile in pipe flows, channel flow or boundary layer (Dubrulle *et al.*, 2001), see Fig. 7.

5 Summary

We have shown in this review that singularities or at least quasi-singularities are likely to be present in flow over boundaries. Taking them into account allows to interpret many of their mysterious features such as dissipation anomaly or small scale vorticity creation via symmetry breaking mechanisms infered from the Navier-Stokes equations. Moreover, they can be used to build new toy model of shear flows, exploiting the spatial intermittency and the scale separation between the large-scale flow and the small-scale structures. The model is very sparse, as only the most intense structures are considered, that are modeled via vortons, representing dynamically regularized quasi-singularities subject to rapid distorsion by the large-scale shear, and which retroact on this large-scale flow via the subgrid stress. The model reproduces the transition between a laminar regime, in which all the dissipation is accounted for by the large-scale flow, and the vortons dynamics is essentially diffusive and a turbulent regime, in which most of the dissipation is produced by the vortons. These two regimes correspond to different scalings of the dissipation and also explain the log-normality of the energy dissipation statistics.

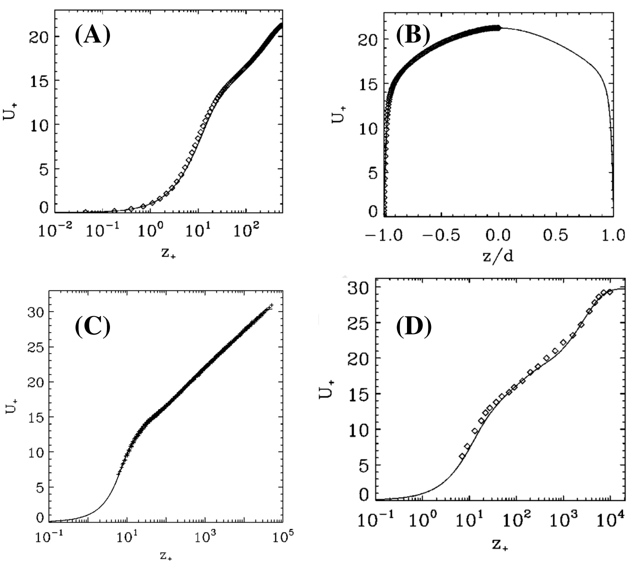

Figure 7. Velocity profile (A) and (B) in a channel flow at $Re = 587.19$: Data of Moser *et al.* (1999) (symbol), analytical model (line). (A) Near the boundary layer. (B) In the bulk. (C) In the Princeton super pipe at 26 value of R_+ between $3.15E+04$ and $3.52E+07$ Data of Zagarola & Smits (1998) (symbols), analytical model (line).($R_* = 14.5$, $K = 0.45$ et $\eta = 0$) ;(D) In a boundary layer at $Re = 20\,920$: Data of Nockemann *et al.* (1994) (symbol), analytical model (line). Credits Dubrulle *et al.* (2001).

In simple cases, the model can also be integrated analytically, provided the quasi-singuarities are regularized into localized Gaussian wave-packets of vorticity. In that case, the $x-z$ component of the subgrid stress tensor scales inversely with the local large-scale shear, leading to the log-law of the wall after integration (Nazarenko, 2000; Nazarenko *et al.*, 2000; Dubrulle *et al.*, 2001). Other interesting generalizations involve more general geophysical flows, and especially localized extreme events such as convective storms. Indeed, individual convective cells are relatively sparse, and move within the "synoptic" (large-scale) wind and temperature fields, while interacting with nearest neighbors. If conditions are favorable, they can further organize into clusters known as mesoscale convective systems (Houze, 2018), which can produce significant hazard. An example of such severe storms are "derechos" which are long-lived MCS producing widespread severe surface wind gusts (Fery & Faranda, 2024). To deal with convective systems, one needs to add the coupling between temperature and velocity, as well as moisture effect. Work is currently in progress to generalize our model to describe such type of coherent structures.

REFERENCES

Bandak, Dmytro, Mailybaev, Alexei A., Eyink, Gregory L. & Goldenfeld, Nigel 2024 Spontaneous stochasticity amplifies even thermal noise to the largest scales of turbulence in a few eddy turnover times. *Phys. Rev. Lett.* **132**, 104002.

Campolina, Ciro S 2022 Fluid dynamics on logarithmic lattices. PhD thesis, IMPA.

Campolina, C. S. & Mailybaev, A. A. 2018 Chaotic blowup in the 3d incompressible euler equations on a logarithmic lattice. *Phys. Rev. Lett.* **121**, 064501.

Campolina, Ciro S. & Mailybaev, Alexei A. 2025 Logarithmic lattice models for flows with boundaries. *Physica D: Nonlinear Phenomena* **472**, 134473.

Collot, Charles, Ghoul, Tej-Eddine, Ibrahim, Slim & Masmoudi, Nader 2022 On singularity formation for the two dimensional unsteady prandtl system around the axis .

Collot, Charles, Ghoul, Tej-Eddine & Masmoudi, Nader 2021 Singularities and unsteady separation for the inviscid two-dimensional Prandtl's system. ArXiv:1903.08244 [math].

Dubrulle, B., Laval, J. P., Nazarenko, S. & Kevlahan, N. K.-R. 2001 A dynamic subfilter-scale model for plane parallel flows. *Physics of Fluids* **13** (7), 2045–2064.

Duchon, Jean & Robert, Raoul 2000 Inertial energy dissipation for weak solutions of incompressible euler and navier-stokes equations. *Nonlinearity* **13** (1), 249.

Eyink, Gregory L. 2006 Turbulent cascade of circulations. *Comptes Rendus Physique* **7** (3), 449–455, statistical mechanics of non-extensive systems.

Eyink, Gregory L. & Drivas, Theodore D. 2015 Spontaneous stochasticity and anomalous dissipation for burgers equation. *Journal of Statistical Physics* **158**, 386–432.

Falkovich, G., Gawędzki, K. & Vergassola, M. 2001 Particles and fields in fluid turbulence. *Rev. Mod. Phys.* **73**, 913–975.

Fery, L. 2025 From coherent structures to convective storms: statistical, observational and modelling approaches to turbulent flows. PhD thesis, University Paris-Saclay, Gif sur Yvette, France.

Fery, Lucas & Faranda, Davide 2024 Analysing 23 years of warm-season derechos in France: A climatology and investigation of synoptic and environmental changes. *Weather and Climate Dynamics* **5** (1), 439–461.

Gargano, F., Sammartino, M., Sciacca, V. & Cassel, K.W. 2014 Analysis of complex singularities in high-reynolds-number navierstokes solutions. *Journal of Fluid Mechanics* **747**, 381421.

Houze, Robert A. 2018 100 Years of Research on Mesoscale Convective Systems. *Meteorological Monographs* **59** (1), 17.1–17.54.

Lellouche, J.-M., Le Galloudec, O., Greiner, E., Garric, G., Regnier, C., Drevillon, M., Bourdall-Badie, R., Bricaud, C., Drillet, Y. & Le Traon, P.-Y. 2018 The copernicus marine environment monitoring service global ocean 1/12 physical reanalysis glorys12v1: Description and quality assessment. In *Egu general assembly conference abstracts*, p. 19806.

Lopez, A. 2026 Exploration of mechanisms leading to turbulent bifurcations. PhD thesis, University Paris-Saclay, Gif-sur-Yvette, France.

Lopez, Adrien & Dubrulle, Bérengère 2026 Viscous and inviscid boundary layers on logarithmic lattices. *preprint* .

Mailybaev, Alexei A. 2016 Spontaneous stochasticity of velocity in turbulence models. *Multiscale Modeling & Simulation* **14** (1), 96–112.

Mailybaev, Alexei A. & Raibekas, Artem 2023 Spontaneous stochasticity and renormalization group in discrete multi-scale dynamics. *Communications in Mathematical Physics* **401** (1), 2643–2671.

Miller, L. 2025 Turbulence regimes along the western boarder of ocean gyres. PhD thesis, ENS Lyon, Lyon, France.

Moser, R.D., Kim, J. & Mansour, N.N. 1999 Direct numerical simulation of turbulent channel flows up to $re_\tau = 590$. *Phys. Fluids* **11**, 943.

Nazarenko, S. 2000 Exact solutions for near-wall turbulence theory. *Physics Letters A* **264** (6), 444–448.

Nazarenko, S., Kevlahan, N. K. R. & Dubrulle, B. 2000 Nonlinear RDT theory of near-wall turbulence. *Physica D: Nonlinear Phenomena* **139** (1), 158–176.

Nockemann, M., Schober, M., Bruns, J., Abstient, R. & Eckert, D.W. 1994 Vermessung der wangrenzschicht im deutsch-niederländischen windkanal bei hohen reynoldszahlen. Technical report. Abhln. Aerodynamisches Institut RWTH, Aachen Heft 32.

Novikov, E. A. 1983 Generalized dynamics of three-dimensional vortex singularities (vortons). *Zhurnal Eksperimentalnoi i Teoreticheskoi Fiziki* **84**, 975–981.

Obabko, A. V. & Cassel, K. W. 2002 Navier-stokes solutions of unsteady separation induced by a vortex. *Journal of Fluid Mechanics* **465**, 99130.

Pearson, Brodie & Fox-Kemper, Baylor 2018 Log-normal turbulence dissipation in global ocean models. *Phys. Rev. Lett.* **120**, 094501.

Prandtl, L. 1905 ber flssigkeitsbewegung bei sehr kleiner reibung. In *Verhandlungen des dritten Internationalen Mathematiker-Kongresses: vom 8. bis 13. August 1904* (ed. A. Krazer), p. 484491. Heidelberg.

Ruffenach, Wandrille, Fery, Lucas & Dubrulle, Bérengère 2025 Toy model of turbulent shear flow using vortons. *Phys. Rev. Fluids* **10**, 054601.

Saint-Michel, Brice, Dubrulle, Bérengere, Marié, Louis, Ravelet, Florent & Daviaud, François 2013 Evidence for forcing-dependent steady states in a turbulent swirling flow. *Phys. Rev. Lett.* **111** (23), 234502.

Thalabard, S., Bec, J. & Mailybaev, A. A. 2020 From the butterfly effect to spontaneous stochasticity in singular shear flows **3** (1), 122.

Zagarola, Mark V. & Smits, Alexander J. 1998 Mean-flow scaling of turbulent pipe flow. *Journal of Fluid Mechanics* **373**, 33 – 79.